Second Order Analysis for Shock Vorticity Wave Interaction

Pranav Thakare, Krishnendu Sinha, Vineeth Nair
Indian Institute of Technology Bombay, Powai, Mumbai, 400076, India
krish@aero.iitb.ac.in, vineeth@aero.iitb.ac.in

Abstract

In this paper, we study the interaction of 2D vorticity waves with a normal shock which is an elementary problem in linear interaction analysis (LIA) theory. The shock refracts the vorticity wave and generates additional acoustic and entropy waves in the downstream flow. The characteristics of the downstream waves are a function of upstream wave amplitude, wave orientation, and Mach number. Our main motive here is to quantify the non-linear effects outside the limits of LIA as a function of these basic parameters theoretically. We perform high order accurate numerical simulations of the full non-linear Euler equations for this problem. RMS error(σ) for the deviation between LIA and high order numerical solution is studied. Results are presented with respect to the variation in fluctuation intensity, wave orientation, and Mach number. The σ is observed to increase with an increase in fluctuation intensity, wave orientation, and Mach number. We present a weakly non-linear analysis of the vorticity amplification at the shock wave. Predictions from the analysis are found to agree with σ variation for the given set of parameters. The results from the analysis for vorticity are used to corroborate the observations. Using weakly non-linear analysis, we discovered σ to scale with the square of the mean compression ratio across the shock for a given upstream orientation of the elementary waves.

1 Introduction

Small intensity fluctuations in the compressible turbulence can be expressed using three fundamental modes[1]. These are vorticity mode, entropy mode and acoustic mode. A theoretical method which uses this decomposition to study the interaction of turbulence with shock wave is known as a linear interaction approach(LIA). Moore [2] and Ribner [3] independently laid the base of LIA theory several decades back. Using Kovasznay[1] mode decomposition, Moore [2] studied the unsteady interaction of an acoustic wave with a normal shock, and Ribner [3] investigated the interaction of a vorticity wave with a normal shock.

LIA is a linear and inviscid theory, which uses concepts from wave physics to study the interaction between flow disturbance and normal shock. It assumes the shock wave to act as a gas-dynamic discontinuity in the flow. Analysis of a single vorticity wave disturbance interacting with a shock is an elementary problem to understand the shock-turbulence interaction. Disturbances in vorticity with some orientation, on interaction with the shock produce wave disturbances in all three modes. Due to non-linear effects, LIA predictions deviate from DNS as the intensity of fluctuations increases. The question as to within what range of governing parameters for which the results from LIA can be considered reliable is still open [4]. This question has become particularly relevant in recent times, where LIA is increasingly being used as a surrogate to numerical simulation in regions of shock waves [5], and LIA-based turbulence models are increasingly being used in practical applications [6, 7, 8]. Hence it is worth exploring the issue introduced. Quantification of the bounds of LIA as a function of basic parameters lacks in the literature. Lack of methodology to quantify the non-linear effects in itself shows the difficulty of the problem. We recognize this gap in the literature and elucidate it using the fundamental problem of shock-vorticity wave interaction.

2 Methodology

We consider a two-dimensional planar vorticity wave being convected by a one dimensional uniform mean flow of velocity $\overline{U}_1$ towards the normal shock located parallel to the y-axis. ϵ and ω denotes the amplitude and temporal frequency of upstream velocity fluctuations, respectively. The position of the unsteady shock deforemed due to impinged vorticity fluctuation is given by the function $\xi(y,t)$.

The incident vorticity wave refracts, whereas acoustic and entropy waves get generated at the shock. α^p,$\vec{k^p}$ and $\vec{k^s}$, α^s represent inclination and wavenumber vector of the generated acoustic wave and the vorticity/entropy wave in the downstream region, respectively. The refracted vorticity wave has the same inclination as that of the entropy wave. The post-shock acoustic wave can be either propagating or decaying depending if angle of the incident wave. There exists a critical angle, α_c for $\alpha \in [0, \pi/2]$, beyond which the acoustic waves decay immediately behind the shock.

The linearized Euler equations with the linearized Rankine-Hugoniot (R-H) conditions as the boundary conditions at the shock are solved to obtain post-shock wave characteristics.The linearized R-H conditions relating the downstream fluctuations in terms of upstream fluctuations are substituted in the linearized Euler equations to obtain the transfer coefficients (Z_{vv}, Z_{vx}, Z_{vp} and Z_{vs}) of the disturbance waves for the region behind the shock. The transfer coefficients are functions of the shock strength (M_1), incidence angle (α), and the adiabatic index (γ).

Two-Dimensional uniform flow is considered upstream and downstream of the shock. We decompose the flow field into mean (zeroth order) and fluctuations using classical Reynolds decomposition ($U = \overline{U} + u'$). For the case considered here, vorticity fluctuations are to be written as

$$\Omega' = \frac{\partial v'}{\partial x}, \tag{1}$$

since the gradients in the shock normal direction are much more significant compared to the gradients in the shock parallel direction.

In order to obtain the gradient of shock parallel velocity fluctuations, the Euler equation for $\boldsymbol{y}$-momentum is decomposed into the mean and fluctuating part using Reynolds decomposition. Terms up to the second-order in ϵ are retained, and expressions with order higher than that are neglected. We define the vorticity fluctuations as $\Omega' = \Omega'_1 + \Omega'_2 + ... + \Omega'_n$, where Ω'_1, Ω'_2, Ω'_n represent the first, second and n^{th} order vorticity fluctuations respectively. Most of the contribution to higher-order vorticity fluctuations come from the terms with a gradient in $\boldsymbol{x}$-direction. Hence the contribution from terms with a gradient in $\boldsymbol{x}$-direction is considered for further analysis.

We carry out the order of magnitude analysis for the variation of all the terms with the gradient in $\boldsymbol{x}$-direction, and from the analysis, the most significant term which could be used to approximate all the second-order non-linear effects in vorticity is found to be

$$\Omega_2' \approx \left(\frac{u_1'}{\overline{U}_2} \frac{\partial v_1'}{\partial x} - \frac{u_2'}{\overline{U}_2} \frac{\partial v_2'}{\partial x} \right) = - \left[\frac{u_i}{\overline{U}_2} \frac{\partial u_i}{\partial x_j} \right]_1^2, \tag{2}$$

2.1 Numerical Methodology

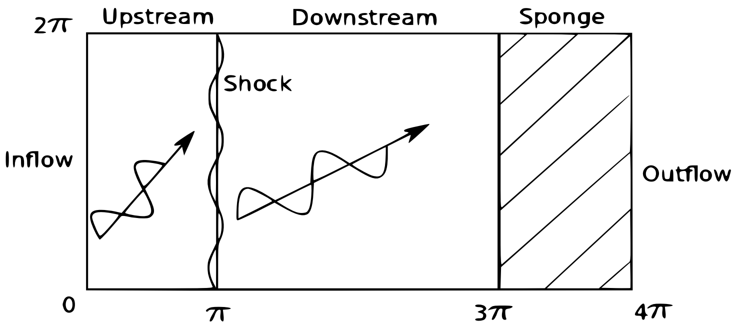

Figure 1: Numerical Domain, station 1: shows the inlet boundary, station-2: initial position of the normal shock, station-3: start of a numerical sponge, station-4:outlet boundary and the end of a numerical sponge

The compressible Euler equations for the interaction vorticity wave and a normal shock (perfect gas, $\gamma = 1.4$) are solved for the upstream Mach number, $M_1 = 1.25, 1.5$ and 1.75 respectively. 5^{th} order accurate WENO scheme with Roe-flux splitting is used to calculate the approximate fluxes near the shock whereas, 6^{th} order accurate central difference scheme is used for the remainder of the domain.

A 2-D computational domain spans 4π streamwise and 2π in the transverse, as shown in Figure 1. A grid size of 800×128 is found to be grid independent and is used for all the cases considered here. The supersonic and non-reflecting subsonic boundary condition is used at the inflow ($x = 0$) and outflow ($x = 4\pi$). The periodic boundary condition is used in the transverse direction. Numerical shock is captured using a modified Ducros sensor[9]. A numerical sponge is used to avoid the reflections from the domain boundaries, which dampens the fluctuations to a target state defined by the Rankine-Hugoniot conditions. In this numerical domain, a numerical sponge appears from position 3π to 4π. A time-dependent back pressure controller is used to keep the shock stationary in the domain similar to the procedure used in [9, 10]. Flow variables are normalized, such that the upstream velocity equals to the upstream Mach number (M_1).

3 Results and discussion

A measure of the deviation of LIA from numerical simulation is studied using the idea of root mean square error (σ). The RMS error is calculated at a position($\boldsymbol{x}$) just downstream of the shock. It is expressed as,

$$\sigma = \sqrt{\frac{1}{N_y N_t}\sum_{n=1}^{N_t}\sum_{n=1}^{N_y}(\Omega'_{NS} - \Omega'_{LIA})^2}, \tag{3}$$

where Ω'_{NS} and Ω'_{LIA} represent the non-dimensional vorticity fluctuations obtained from the NS and LIA, respectively. Here, N_y is the number of grid points in y direction at a given x location used to compute the σ in the downstream region, and N_t represents the number of time instants. Total number of grid points were found to be sufficiently large for statistical convergence.

σ implies the quantification of non-linear effects in the numerical simulations, which LIA theory does not consider. It denotes the primary source of error in LIA for ϵ, α, and M_1. A theoretical measure of Ω'_2 is derived from the equation 2 to predict the non-linear effects. Now we compare the σ and Ω'_2 variation for ϵ and M_1 at $\alpha = 20°$ and $\alpha = 30°$, respectively.

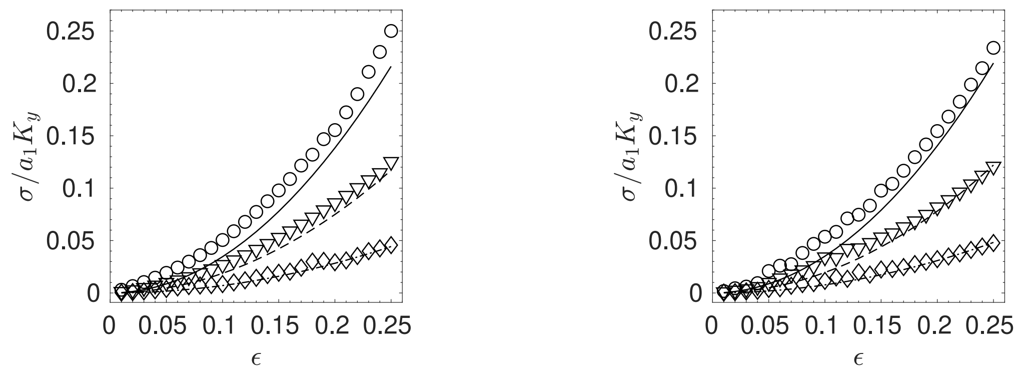

(a) $\alpha = 20°$

(b) $\alpha = 30°$

Figure 2: Variation of σ(symbols) and Ω'_2 (line) respectively with respect to ϵ at $M_1 = 1.25$(diamond symbol and dotted dashed line), $M_1 = 1.5$ (triangle symbol and dashed line) and $M_1 = 1.75$ (circle symbol and solid line) for (a)$\alpha = 20°$, (b)$\alpha = 30°$

It is observed that the σ value rises with an increase in ϵ and M_1 for a given α. The variation of σ with respect to ϵ is noticed be of the higher-order, and besides that the variation of Ω'_2 also shows the increasing trend for ϵ and M_1 at given α. On comparison with Ω'_2, we discovered that the variation of σ for ϵ at all the M_1 and α is of second order.

The non-linear effects are triggered at a higher ϵ and M_1 due to the modal interaction for a given α. It likewise reflects the validation of the prediction of modal interaction made by Chu[11] with a problem involving the shock wave for the first time. Ω'_2 from the weakly non-linear analysis predicts the deviation (σ) and for that matter, non-linear effects precisely and thus validate the prediction of weakly non-linear analysis.

3.1 Scaling of the error

We asserted that the weakly non-linear theory captures the non-linear effects due to ϵ variation at a given α and M_1. In this section, we analyse the scaling behaviour of σ with respect to different M_1.

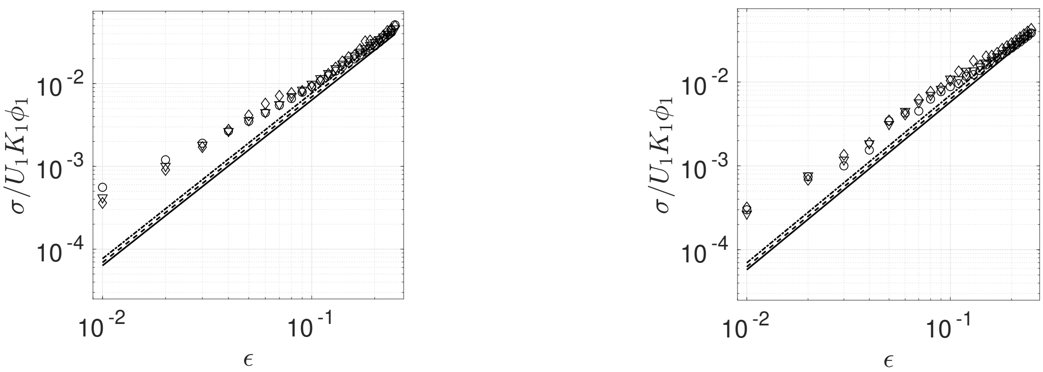

(a) $\alpha = 20°$

(b) $\alpha = 30°$

Figure 3: Variation of scaled σ(symbols) with respect to ϵ at $M_1 = 1.25$(diamond symbol and dotted dashed line), $M_1 = 1.5$ (triangle symbol and dashed line) and $M_1 = 1.75$ (circle symbol and solid line) for (a)$\alpha = 20°$, (b)$\alpha = 30°$

In the previous section, we approximated all the non-linear effects in Ω_2' as represented in equation 2. Using the Fabre's representation, Ω_2' is given as

$$\Omega_2' = -\underbrace{r\sin\alpha\cos^2\alpha}_{\phi_{11}} + \underbrace{\frac{\sin\alpha}{r}\left(\sin\alpha^s Z_{vv} + \frac{\cos\alpha^p Z_{vp}}{\gamma M_2 \xi}\right)\left(\frac{\cos^2\alpha^s}{\sin\alpha^s} Z_{vv} - \frac{\cos\alpha^p Z_{vp}}{\gamma M_2\xi}\right)}_{\phi_{12}}. \quad (4)$$

ϕ_{11} and ϕ_{12} are the sub-terms of Ω_2' from equation 2. We perceive that the ϕ_{11} varies as $\boldsymbol{r}$ and the ϕ_{12} varies as r^2 with respect to M_1 for a given α

From the order of the magnitude analysis, we noticed that the variation of ϕ_{11} and ϕ_{12} combined with respect to M_1 goes approximately as $f(r^2, \alpha)$, where r represents the ration of mean velocity across the shock. Therefore, equation 2 from the last section can be modified to

$$\frac{\Omega_2'}{i\overline{U}_1 K_1} \approx \epsilon^2 r^2 f(\alpha). \quad (5)$$

The equation 5 signifies that the variation of Ω_2' (from 2) with respect to M_1 can be approximated as the $f(r^2, \alpha)$. r^2 being an explicit function of M_1; the scaling of the σ is a strong function of M_1. To verify that, we divide normalized σ and σ_T by Ω_2' and study its scaling behavior.

Figure 3a and 3b shows the variation of σ and σ_T with respect to ϵ as divided by r^2 at $\alpha = 20°$, and $30°$, respectively. We observe that the σ and Ω_2' variation collapses to a single curve for all the M_1 when scaled by r^2 approximately. However, at lower M_1, ($M_1 = 1.25$) σ is not collapsed completely on the other σ variations ($M_1 = 1.5, 1.75$) and the similar behavior is observed with the Ω_2'. This behaviour could be ascribed to the order of magnitude analysis, which is more accurate for the higher M_1 at a given α. We state that the r^2 scaling for the variation of σ due to non-linear effects works nicely at all the M_1 for a given α except very close to the sonic limit. On using measures form the weakly non-linear theory and the scaling, departure in the LIA results from the numerical simulation can be corrected to obtain a more accurate solution.

The weakly non-linear theory presented here is for the interaction of vorticity wave with a normal shock in the propagative regime and the scaling obtained is for vorticity fluctuations downstream of the shock. With similar analysis, scaling could be found for the acoustic and entropy fluctuations downstream of the shock. Understanding acquired from this study could be used to build a more robust and critical theory for practical problems such as shock-turbulence interaction, shock boundary-layer interaction, flame-turbulence interaction, and related problems.

4 Conclusion

The interaction of vorticity wave with a normal shock is investigated theoretically as well as numerically at the various ϵ, M_1 and α, respectively. A second-order weakly non-linear analysis is presented for the vorticity fluctuations downstream of the shock. A most important second-order term which approximates for all the non-linear effects due to modal interaction is identified using order of magnitude analysis. Higher-order accurate numerical simulations are performed for shock vorticity interaction at a provided governing parameters. A parameter termed σ defined based on the deviation between the results from LIA and numerical simulations found to be good measure to comprehend the deviation between LIA and numerical simulations. Comparison of RMS of Ω_2' from theory and σ for $\epsilon = 1\%$ to 25%, and $M_1 = 1.25, 1.5, 1.75$ at $\alpha = 20°, 30°$ is carried out. We found that the variation of Ω_2' and σ follows a similar trend. It confirms that second-order weakly non-linear analysis presented here can capture the non-linear effects due to modal interactions. Scaling behaviour of σ with respect to M_1 is examined using the expressions from the weakly non-linear analysis. We found that σ scales approximately as a square of the ration of mean velocity across the shock, i.e. r^2. The obtained scaling could be used to improve the results from LIA theory at higher ϵ.

References

[1] S. G. Kovasznay, J. Aeronautic. Sci. **Vol-23**, 10(1953)

[2] F. K. Moore, NACA TR 1165, **217** (1954)

[3] H. S. Ribner, AIAA J. **23**, 1708(1985)

[4] C. Chen, D. Donzis , J. Fluid Mech. **Vol-870**, 813-847(2019)

[5] N. O. Braun et al., *Large eddy simulation investigation of the canonical shock-turbulence interaction*, J. Fluid Mech. **858**, 500 (2019)

[6] K. Sinha, et al., *Modeling shock unsteadiness in shock turbulence interaction*,Phys. Fluids. **Vol-15**(2003)

[7] K. Sinha, et al., *Modeling the Effect of Shock Unsteadiness in Shock-Turbulent Boundary-Layer Interactions*, AIAA J. **Vol-43**(2005)

[8] S. Roy, et al.,*Variable turbulent Prandtl number model for shock-boundary layer interaction*, AIAA J. **Vol-56**(2018)

[9] J. Larsson et al., *Reynolds-and Mach-number effects in canonical shock-turbulence interaction*, J. Fluid Mech. **717**, 293 (2013)

[10] Y. P. M. Sethuraman et al., *Thermodynamic fluctuations in canonical shock–turbulence interaction: effect of shock strength*, Theor. Comput. Fluid Dyn., **32**, 629 (2018)

[11] B. T. Chu, L. S. G. Kovásznay, J. Fluid Mech. **3**, 494 (1958)